Microscopic Origin of Large Negative Magnetoelectric Coupling in $Sr_{1/2}Ba_{1/2}MnO_3$

Gianluca Giovannetti,[1,2] Sanjeev Kumar,[3] Carmine Ortix,[2] Massimo Capone,[1] and Jeroen van den Brink[2]

[1]*CNR-IOM-Democritos National Simulation Centre and International School for Advanced Studies (SISSA), Via Bonomea 265, Trieste I-34136, Italy*

[2]*Institute for Theoretical Solid State Physics, IFW-Dresden, PF 270116, Dresden, Saxony 01171, Germany*

[3]*Indian Institute of Science Education and Research(IISER) Mohali, Knowledge City, Sector 81, Mohali, Punjab 140306, India*

(Received 8 February 2012; published 7 September 2012)

With a combined *ab initio* density functional and model Hamiltonian approach we establish that in the recently discovered multiferroic phase of the manganite $Sr_{1/2}Ba_{1/2}MnO_3$ the polar distortion of Mn and O ions is stabilized via enhanced in-plane Mn-O hybridizations. The magnetic superexchange interaction is very sensitive to the polar bond-bending distortion, and we find that this dependence directly causes a strong magnetoelectric coupling. This novel mechanism for multiferroicity is consistent with the experimentally observed reduced ferroelectric polarization upon the onset of magnetic ordering.

DOI: 10.1103/PhysRevLett.109.107601 PACS numbers: 77.80.−e, 71.10.−w, 71.27.+a, 71.45.Gm

Multiferroic materials are ideal candidates for the realization and practical use of strong magnetoelectric (ME) effects [1,2]. The scarcity of actual materials that are magnetic ferroelectrics appears to be related to the competition between the conventional mechanism of ferroelectric cation off-centering, which requires empty *d* orbitals, and the formation of magnetic moments which requires partially filled *d* orbitals [1,2]. A concomitance of magnetism and ferroelectricity and in particular its interplay in homogeneous systems then has to rely on more subtle microscopic coupling mechanisms, driven by spin-orbit coupling in the form of Dzyaloshinskii-Moriya interactions [3] or exchange-striction [4]. Such coupling mechanisms also underly the switching of multiferroic domain structures as observed in for instance $BiFeO_3$ [5]. The recently synthesized manganite $Sr_{1/2}Ba_{1/2}MnO_3$ (SBMO) however, defeats the generic incompatibility of a cation both having a magnetic moment and being ferroelectrically displaced. Therefore the ME coupling in SBMO is expected to be much stronger compared to, for example, $BiFeO_3$, where the Bi lone pair is responsible for ferroelectricity and the Fe ion for magnetism. SBMO thus provides a classic example of a material in which charge, spin, lattice, and orbital degrees of freedom are strongly coupled, giving in this particular case rise to a strong ME effect, the origin of which we set out to clarify here.

For doing so, the methods from modern *ab initio* band structure theory are powerful tools—very helpful not only in predicting new multiferroic materials, but also in understanding the underlying mechanisms for ME couplings. The computed values of macroscopic polarization *P* agree well with those observed experimentally [6–14]. In the last few years several *ab initio* calculations have pointed out the possible ferroelectric state with a large polarization for $AMnO_3$, where *A* is an alkaline earth element. The proposed mechanism is based on off-centering of Mn^{4+} ions stabilized via a charge-lattice coupling of Peierls type [15–17]. The problems in synthesizing such a material with predicted ferroelectricity have very recently been overcome: last year SBMO was reported to support a ferroelectric phase via the off-centering of magnetic Mn^{4+} ion in conjunction with a perovskite tetragonal structure [18]. The onset of the low-temperature long-range antiferromagnetic (AFM) ordering strongly reduces the polarization indicating a large ME effect [18]. The AFM order, in other words, does not support ferroelectricity, but it neither completely destroys it. This special feature of SBMO opens a new avenue for the quest of materials with strong ME effects, where the search need not be restricted to systems in which ferroelectricity and magnetism mutually stabilize each other.

Here we establish with a combination of first-principles calculations and a model Hamiltonian analysis that the ferroelectric polarization mainly arises from a polar distortion of Mn and O ions caused by an enhanced in-plane Mn-O hybridization. Since the magnetic superexchange interaction strongly depends on this distortion, a strong and novel type of ME coupling arises. This ME coupling is negative in the sense that the ferroelectric polarization is not promoted by magnetism, but rather reduced by it, which renders AFM ordering and ferroelectricity strongly coupled.

We first present the results of our first-principles calculations based on density functional theory [19] using the generalized gradient approximation (PBE) [20] and including correlation effects within the DFT + *U* scheme [21] as implemented in VASP [22]. We use on-site Coulomb and exchange parameters $U = 3.0$ and 4.5 eV and $J_H = 1.0$ eV on the manganese *d* orbitals. In the projector augmented wave scheme [23] the cutoff for the plane-wave basis set was chosen as 400 eV and an $8 \times 8 \times 8$ mesh was used for the Brillouin-zone sampling. To calculate the electronic contribution to the spontaneous polarization we use the

Berry-phase method developed by King-Smith and Vanderbilt [24]. In the calculations, the in-plane lattice constant is taken as $a = 3.85$ Å. For the interplane distance we consider the two values $c/a = 1.005$, 1.01, which are experimentally determined for the SBMO at different temperatures [18].

For all the above parameters SBMO is safely in an AFM (G-type) insulating state with a band gap of $\sim$0.4 eV with Mn magnetic moments $M \sim 2.6\mu_b$, in agreement with previous density functional theory calculations on $CaMnO_3$ and $SrMnO_3$ [16,17,25] and experiments on $SrMnO_3$ [26]. The valence band is predominantly majority-spin Mn t_{2g} and O 2p character with strong p-d hybridization while the conduction band is formed by the Mn e_g orbital and empty minority t_{2g} states, which is consistent with Mn^{4+} in an octahedral crystal field. To find the energetically most stable configuration we relax the ions performing structural optimization in a 40 atoms $2 \times 2 \times 2$ unit cell. We start the relaxation from a checkerboard arrangement of the Sr, Ba ions and check that our results do not depend on this assumption.

Even if the initial ionic structure belongs to space group $I4/mmm$ (No. 139) which is centrosymmetric, for all our parameters, the relaxed structure belongs to the space group $I4mm$ (No. 107) and it breaks inversion symmetry. The polar ionic displacements associated with the reduced symmetry are shown schematically in Fig. 1. The O-Mn-O angle α (see Fig. 1) which is 180° for ideal centrosymmetric structure with $c/a = 1$, is reduced in agreement with the experimentally determined low symmetry structure [18]. The deviation of α from 180° as a function of c/a is shown in Fig. 2. We now analyze the effect of this reduced angle on the ferroelectric polarization. We first notice that the electronic contribution to the spontaneous polarization P evaluated in the centrosymmetric structures ($I4/mmm$) for the AFM ground state is zero, meaning that the polar state is not magnetically driven. Indeed at different values of the ratio c/a it is the covalent bond formation upon ionic displacements between e_g orbitals of Mn and p orbitals of apical O ions that stabilizes the ferroelectric state [16].

On the other hand in the relaxed state, the large polar displacements of the apical O ions along the c lattice direction result in the formation of dipolar pairs between manganese and oxygen (see Fig. 1) and in a state similar to a bond-centered charge density wave [27]. At low temperature, when the system orders antiferromagnetically, this enables the practical realization of a peculiar and atypical multiferroic state. This is shown by the results for the polarization P, whose electronic and ionic contributions (P_{ele}, P_{ionic}) are plotted in Fig. 2. Increasing the ratio c/a from 1.005 to 1.01, the magnitude of the electronic contribution P_{ele} increases and that of the ionic contribution P_{ionic} decreases. The total polarization $P = P_{\text{ele}} + P_{\text{ionic}}$, however, increases from $c/a = 1.005$ to $c/a = 1.01$. The ionic contribution is calculated as $P_{\text{ionic}} = \sum_i Z_i ds_i$, where Z_i is the nominal rigid core charge of the ith-ion and ds_i is the displacement of the ith ion. The sum is over all ions present in the unit cell. Since $P_{\text{ionic}} = 0$ at $c/a = 1$, it behaves nonmonotonically with increasing c/a. The calculated value of P agrees with the experimental value of 13.5 μC/cm^2 for the single domain [18]. This physical result does not depend strongly on the structural and interaction (U, J_H) parameters, but the quantitative description of the ferroelectric instability in SBMO should of course depend on the actual values of these parameters, as has been found to be the case in other Mn based multiferroic materials [10]. In particular, at larger U the magnetic moment increases and the ferroelectric tendency decreases as the angle α gets closer to 180° (see Fig. 2).

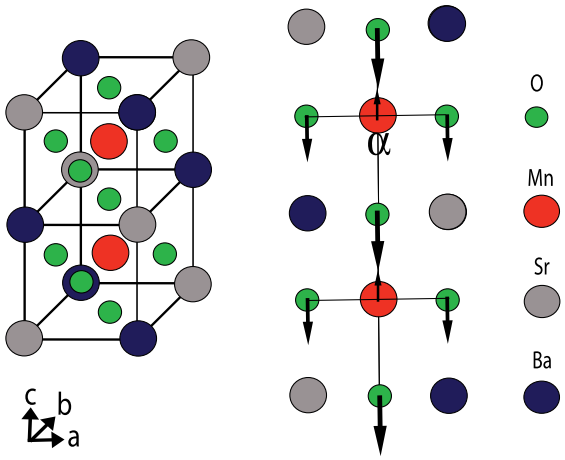

FIG. 1 (color online). (Color online) Schematic view of a SBMO unit cell and displacements of Mn and O sites in AFM magnetic structure. Arrows indicate the relative atomic ferroelectric displacements.

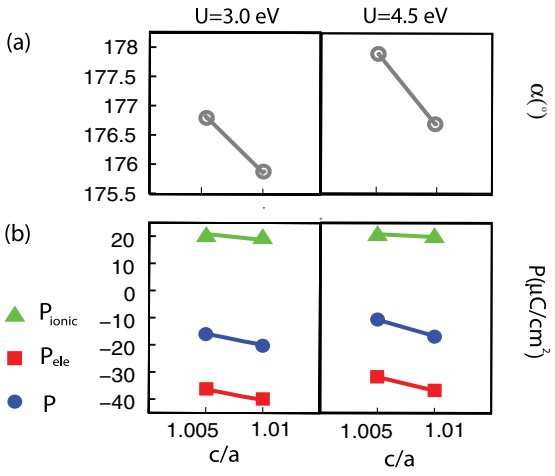

FIG. 2 (color online). (Color online) (a), (b) Variation of the O-Mn-O angle α and spontaneous polarization P, P_{ele}, P_{ionic} with the ratio c/a for $U = 3.0$ and 4.5 eV, respectively.

The calculated polarizations show that the ferroelectric (FE) order is not driven by the magnetic order, but yet the two are strongly coupled. This counterintuitive situation arises, as we will show next, from the ferroelectric transition in SBMO being driven by Mn and O displacement and the mechanism of the suppression of tetragonal distortion below T_N [18] being due to the subsequent strong change in the superexchange interactions betweens Mn spins [28]. The 180° O-Mn-O bonds are energetically favored by the AFM coupling [28] then in the ferroelectric state the off-centering of Mn ions, which is in favor of the inset of double exchange interactions, gets suppressed with a net decrease of the ferroelectric polarization [29]. The effect of the magnetism on the ferroelectric distortions can be captured by performing calculations with noncollinear magnetic structures having Mn spins with angle θ ranging from 0° (G-type) to 90° [see Fig. 3(a)] to control how the superexchange interactions along the O-Mn-O bonds change P. At each angle θ the lattice structure is relaxed and the sum of electronic and ionic contributions to the ferrolectric polarization is evaluated [see Fig. 3(b)]. Increasing the angle θ between the spins reduces the superexchange interactions. The Mn-O-Mn angle α decreases with a resulting larger Mn off-centering which stabilizes the ferroelectric polarization. We observe that the magnetic order alters both electronic and ionic contributions to the polarization via a change in α: the magnetism is thus coupled to the lattice and the latter is coupled to the polarization. Increasing the superexchange interactions causes the magnetic structure to drive the lattice towards a recovery of the a centrosymmetric arrangement.

From a phenomenological point of view, the suppression of FE polarization at the onset of AFM ordering implies

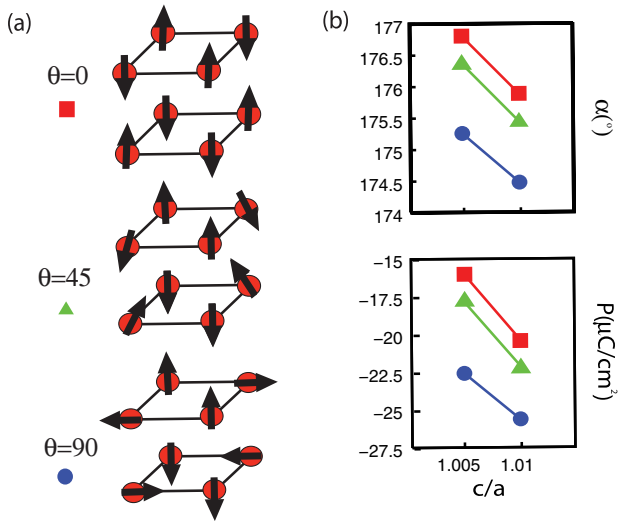

FIG. 3 (color online). (Color online) (a) Schematic view of noncollinear magnetic structures having Mn spins with angle $\theta = 0^o$, 45°, 90°; (b) Variation of the O-Mn-O angle α and spontaneous polarization P with the ratio c/a for different values of θ at $U = 3.0$ eV and $J_H = 1.0$ eV.

the existence of a positive term in the Landau free energy involving the product of the square of the polarization and the square of the AFM order parameter (see the Supplemental Material [30]). In this case the appearance of a multiferroic phase implies close proximity to a tetracritical point, which is indeed present in the experimental phase diagram of $Sr_{1-x}Ba_xMnO_3$ [18].

To flesh out the microscopic origin of the ferroelectric instability we set up a model Hamiltonian, based on the band structure results and taking into account the different magnetic exchange interactions and the coupling of the electrons to the lattice:

$$H = -\sum_{i,\gamma,\sigma} t^{\gamma}(u_i)(d^{\dagger}_{i,\sigma}p_{i+\gamma,\sigma} + \text{H.c.}) + \sum_i \Delta_{\text{pd}} d^{\dagger}_{i,\sigma} d_{i,\sigma} - J_H \sum_i \mathbf{S}_i \cdot \boldsymbol{\sigma}_i + J_S \sum_{\langle ij \rangle} \mathbf{S}_i \cdot \mathbf{S}_j + K_s \sum_i u_i^2.$$

Here, $d_{i,\sigma}$ ($p_{i,\sigma}$) and $d^{\dagger}_{i,\sigma}$ ($p^{\dagger}_{i,\sigma}$) are the annihilation and creation operators for Mn-d (O-p^z) electrons with spin $\sigma = \uparrow, \downarrow$. $\mathbf{S}_i$ are the localized t_{2g} spins ($S = 3/2$), which in this study are treated classically and coupled antiferromagnetically via J_S. The sum over $\langle ij \rangle$ denotes the sum over nearest neighbor Mn ions. u_i are the off-centering distortions of Mn ions along the c axis and K_s denotes the stiffness energy associated with these distortions. $t^{\gamma}(u_i)$ denote the distortion-dependent hopping amplitudes between $d_{3z^2-r^2}$ and p^z orbitals along γ direction ($\gamma = x, y, z$). Note that γ denotes the direction in real space and not the character of the p orbitals. The σ_i denote the electronic spin operator defined as, $\sigma^{\mu}_i = \sum_{\alpha\beta} d^{\dagger}_{i\alpha} \tau^{\mu}_{\alpha\beta} d_{i\beta}$, where τ^{μ} are the Pauli matrices. Δ_{pd} is the on-site energy difference between Mn-$d_{3z^2-r^2}$ and O-p^z levels.

In the model Hamiltonian the ionic displacements are restricted to the c-axis direction, as observed in the experiments and verified in our band structure calculations. In principle the O ions are easier to displace; however, a combination of O displacements and Mn displacements can be modeled as a net off-centering displacement of the Mn ions along with an overall change in the lattice c parameter. Here, we model the effective displacements via the off-centering $u_i a$ of the Mn ions, where a is the Mn-Mn lattice spacing. We consider only the $d_{3z^2-r^2}$ orbital as the one that can hybridize with the O-p_z levels, since the planar orbitals $d_{x^2-y^2}$ have zero overlap with the O-p_z.

If Mn ions are located at the center of O_6 octahedra then the hopping between $d_{3z^2-r^2}$ and O-p_z is nonzero only along the z axis and is given by $t_0 = (pd\sigma)$. However, if Mn ions are off-centered by a small displacement they lead to a finite in-plane hopping which can be calculated from the Slater-Koster tables as $t^{x/y} = n[n^2 - (l^2 + m^2)/2](pd\sigma) + \sqrt{3}n(l^2 + m^2)(pd\pi)$, where l, m, n are the direction cosines from O to Mn [31]. Taking only the $pd\sigma$ contribution one can write the hopping integral in terms of the Mn-O-Mn angle α as, $t^{x/y} = \sin(\alpha/2)[\sin^2(\alpha/2) - \cos^2(\alpha/2)/2](pd\sigma)$. Rewriting the

trigonometric functions in terms of the the distortions, we get to leading order in the distortion u_0, $t^{x/y} \sim -2u_0(pd\sigma)$. The next order term is $O(u_0^3)$ which can be safely ignored. Naturally t^z_{pd} is also modified via a Peierls-type term with the hopping between longer and shorter bonds given by $t^z_{\pm} = (1 \pm gu)t_0$.

Just as the off-centering of Mn ions affects the hopping parameters t^{γ}_{pd}, it also affects the value of J_S via the Mn-O-Mn bond angle. J_S is maximum at $\alpha = \pi$ and is reduced by any deviation. The leading order change in the Taylor expansion around the point $\alpha = \pi$ is $O(\delta\alpha^2)$. Therefore, for small deviations we can model the distortion-dependence as $J_S^{x/y} = -J_0 \cos(\alpha)$. In principle J_S^z is also affected since the distances Mn-O_1 and Mn-O_2 for the two apical oxygens become unequal, but this dependence does not affect the physical picture.

Given a specific configuration of lattice distortions and t_{2g} spins, one can easily diagonalize the electronic problem numerically on finite lattices. We set $t_0 = 1$, and therefore all other model parameters are in units of t_0. It is important to show that the parameters used in calculations are within the physical range for SBMO. The combined e_g and p^z bandwidth can be estimated as $\sim$2 eV [16], which leads to an estimate for $t_0 \sim 0.2$ eV. The Neel temperature for $SrMnO_3$ is $T_N \sim 260$ K [26]. Therefore we use $J_S = 0.1t_0 \sim 20$ meV. It is difficult to estimate the elastic constant associated with pure off-centering distortion of the Mn ions. However, $K_s = t_0$ is commonly used in models for manganites when dealing with distortions of the O ions. The energy cost involved in off-centering a Mn ion is much larger than that involved in displacing O ions. Therefore we use $K_s = 15t_0$ as an estimate of the elastic energy cost. The ferroelectric and multiferroic phases will be even more stable for a smaller value of K_s. With all these parameters fixed, we explore the ferroelectric and paramagnetic states by varying J_H and Δ_{pd}. Our focus is to explore the possibility of a FE state in both the nonmagnetic and AFM phase. Therefore, rather than performing a lengthy minimization of the energy as a function of classical spin and lattice variables, we compare the total energy of only the relevant configurations. We use the magnitude of off-centering distortions $u(i) \equiv u_0$ as a variational parameter and determine the distortions $u_{\min}$ that correspond to the lowest total energy. A nonzero value of $u_{\min}$ is the hallmark of a FE state. The onset of antiferromagnetism leads to a reduction in the tendency to form a FE state, which is reflected in a reduced value of $u_{\min}$ for the AFM order shown in Fig. 4(a).

The results of the model calculations are summarized in the Δ-J_H phase diagram in Fig. 4(b). The phase diagram shows that the FE phase is stabilized over a wide range of parameter space when the system is in paramagnetic state. The presence of AFM order shrinks the regions of stability of the FE order, and in general the AFM order reduces the value of FE polarization for all parameter values. We present the phase diagram for $g = 0$, which shows that the mechanism for FE ordering does not depend on the Peierls-type electron-lattice coupling. However, the presence of a nonzero g further stabilizes the FE order. Since the FE order is stable in the AFM state in SBMO, the phase diagram in Fig. 4(b) puts upper bounds on parameters J_H and Δ_{pd} as $J_H \leq 6$ and $\Delta_{pd} \leq 2$. The typical estimates $J_H \sim 1$ eV $= 5t_0$ and $\Delta_{pd} \sim 0.2$ eV $= t_0$ fall inside the FE-AFM phase of the phase diagram.

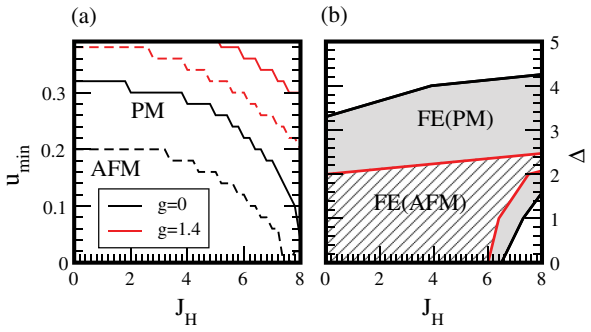

FIG. 4 (color online). (Color online) (a) $u_{\min}$ as a function of J_H for paramagnetic and antiferromagnetic spin configurations for $g = 0$ and $g = 1.4$. The AFM state leads to a reduction in FE distortion. (b) Phase diagram in Δ-J_H phase space showing the regions of FE stability.

In conclusion, by combining different theoretical approaches we highlight the intricate interrelationship between magnetic and ferroelectric orderings in the recently discovered multiferroic phase of $Sr_{1/2}Ba_{1/2}MnO_3$ [18]. The new mechanism at play relies on the distortion dependent in-plane hopping between Mn and O sites and strongly depends on the onset of the magnetic order. Via an interplay between charge, spin, lattice, and orbital degrees of freedom this leads to the experimentally observed magnetically suppressed ferroelectricity. This type of strong ME coupling being present in $Sr_{1/2}Ba_{1/2}MnO_3$ opens new routes for the search of multiferroic materials different from other Mn based oxides such as $RMnO_3$ and RMn_2O_5 [2], going beyond the requirement of the magnetic ordering breaking the inversion symmetry, whereby it causes a ferroelectric instability.

This work is supported by CINECA who allocated computer time. M. C. and G. G. acknowledge financial support by the European Research Council under FP7/ERC Starting Independent Research Grant "SUPERBAD" (Grant Agreement No. 240524). S. K. acknowledges support from DST, India. We thank R. O. Kuzian, S.-L. Drechsler, and J. Malek for stimulating discussions.

[1] N. A. Hill, J. Phys. Chem. B **104**, 6694 (2000).
[2] S. W. Cheong and M. Mostovoy, Nature Mater. **6**, 13 (2007).

[3] H. Katsura, N. Nagaosa, and A. V. Balatsky, Phys. Rev. Lett. **95**, 057205 (2005).
[4] T. Arima, A. Tokunaga, T. Goto, H. Kimura, Y. Noda, and Y. Tokura, Phys. Rev. Lett. **96**, 097202 (2006).
[5] T. Zhao *et al.*, Nature Mater. **5**, 823 (2006).
[6] N. A. Hill, Annu. Rev. Mater. Res. **32**, 1 (2002).
[7] S. Picozzi and C. Ederer, J. Phys. Condens. Matter **21** 303201 (2009).
[8] P. Baettig, C. Ederer, and N. A. Spaldin, Phys. Rev. B **72**, 214105 (2005).
[9] S. Picozzi, K. Yamauchi, B. Sanyal, I. A. Sergienko, and E. Dagotto, Phys. Rev. Lett. **99**, 227201 (2007).
[10] G. Giovannetti and J. van den Brink, Phys. Rev. Lett. **100**, 227603 (2008).
[11] A. Malashevich and David Vanderbilt, Phys. Rev. Lett. **101**, 037210 (2008).
[12] G. Giovannetti, S. Kumar, A. Stroppa, J. van den Brink, S. Picozzi, and J. Lorenzana, Phys. Rev. Lett. **106**, 026401 (2011).
[13] A. Stroppa, M. Marsman, G. Kresse, and S. Picozzi, New J. Phys. **12**, 093026 (2010).
[14] K. Yamauchi, P. Barone, and S. Picozzi, Phys. Rev. B **84**, 165137 (2011).
[15] S. Bhattacharjee, E. Bousquet, and P. Ghosez, Phys. Rev. Lett. **102**, 117602 (2009).
[16] J. M. Rondinelli, A. S. Eidelson, and N. A. Spaldin, Phys. Rev. B **79**, 205119 (2009).
[17] J. H. Lee and K. M Rabe, Phys. Rev. Lett. **104**, 207204 (2010).
[18] H. Sakai *et al.*, Phys. Rev. Lett. **107**, 137601 (2011).
[19] P. Hohenberg and W. Hohn, Phys. Rev. **136**, B864 (1964); W. Kohn and L. J. Sham, Phys. Rev. **140**, A1133 (1965).
[20] J. P. Perdew, K. Burke, and M. Ernzerhof, Phys. Rev. Lett. **77**, 3865 (1996).
[21] A. I. Liechtenstein, V. I. Anisimov, and J. Zaanen, Phys. Rev. B **52**, R5467 (1995).
[22] G. Kresse and J. Furthmuller, Phys. Rev. B **54**, 11169 (1996); G. Kresse and J. Furthmuller, Comput. Mater. Sci. **6**, 15 (1996).
[23] G. Kresse and D. Joubert, Phys. Rev. B **59**, 1758 (1999).
[24] R. D. King-Smith and D. Vanderbilt, Phys. Rev. B **47**, 1651 (1993); D. Vanderbilt and R. D. Smith, Phys. Rev. B **48**, 4442 (1993).
[25] S. Picozzi, C. Ma, Z. Yang, R. Bertacco, M. Cantoni, A. Cattoni, D. Petti, S. Brivio, and F. Ciccacci Phys. Rev. B **75**, 094418 (2007).
[26] T. Takeda and S. Ōhara, J. Phys. Soc. Jpn. **37**, 275 (1974).
[27] G. Giovannetti, S. Kumar, J. van den Brink, and S. Picozzi, Phys. Rev. Lett. **103**, 037601 (2009).
[28] J. B. Goodenough, Phys. Rev. **100**, 564 (1955); J. Kanamori, J. Phys. Chem. Solids **10**, 87 (1959).
[29] J. van den Brink and D. I. Khomskii, J. Phys. Condens. Matter **20**, 434217 (2008).
[30] See Supplemental Material at http://link.aps.org/supplemental/10.1103/PhysRevLett.109.107601 for the Landau theory of the negative magnetoelectric coupling.
[31] J. C. Slater and G. F. Koster, Phys. Rev. **94**, 1498 (1954).